HHS Public Access

Author manuscript

Science. Author manuscript; available in PMC 2018 May 24.

Published in final edited form as:

Science. 2017 November 24; 358(6366): 1027–1032. doi:10.1126/science.aan3456.

Molecular and Cellular Reorganization of Neural Circuits in the Human Lineage*

André M. M. Sousa[1,†], **Ying Zhu**[1,†], **Mary Ann Raghanti**[2], **Robert R. Kitchen**[3,4], **Marco Onorati**[1,5], **Andrew T. N. Tebbenkamp**[1], **Bernardo Stutz**[6], **Kyle A. Meyer**[1], **Mingfeng Li**[1], **Yuka Imamura Kawasawa**[1,7], **Fuchen Liu**[1], **Raquel Garcia Perez**[8], **Marta Mele**[8], **Tiago Carvalho**[8], **Mario Skarica**[1], **Forrest O. Gulden**[1], **Mihovil Pletikos**[1], **Akemi Shibata**[1], **Alexa R. Stephenson**[2], **Melissa K. Edler**[2], **John J. Ely**[9], **John D. Elsworth**[4], **Tamas L. Horvath**[1,6], **Patrick R. Hof**[10], **Thomas M. Hyde**[11], **Joel E. Kleinman**[11], **Daniel R. Weinberger**[11], **Mark Reimers**[12], **Richard P. Lifton**[13,14], **Shrikant M. Mane**[15], **James P. Noonan**[13], **Matthew W. State**[16], **Ed S. Lein**[17], **James A. Knowles**[18], **Tomas Marques-Bonet**[8,19,20], **Chet C. Sherwood**[21], **Mark B. Gerstein**[3], and **Nenad Sestan**[*,1,4,6,13,22]

[1]Department of Neuroscience and Kavli Institute for Neuroscience, Yale School of Medicine, New Haven, Connecticut, USA

[2]Department of Anthropology and School of Biomedical Sciences, Kent State University, Kent, Ohio, USA

[3]Program in Computational Biology and Bioinformatics, Departments of Molecular Biophysics and Biochemistry and Computer Science, Yale University, New Haven, Connecticut, USA

[4]Department of Psychiatry, Yale School of Medicine, New Haven, Connecticut, USA

[5]Department of Biology, Unit of Cell and Developmental Biology, University of Pisa, Pisa, Italy

[6]Program in Integrative Cell Signaling and Neurobiology of Metabolism, Section of Comparative Medicine, New Haven, Connecticut, USA

[7]Departments of Pharmacology and Biochemistry and Molecular Biology, Institute for Personalized Medicine, Penn State University College of Medicine, Hershey, Pennsylvania, USA

[8]Institut de Biologia Evolutiva, CSIC-Universitat Pompeu Fabra, PRBB, Barcelona, Catalonia, Spain

*Correspondence to: Nenad Sestan (nenad.sestan@yale.edu).
†These authors contributed equally to this work.

Data is available at NCBI BioProjects (accession number: PRJNA236446).

List of Supplementary Materials:
Materials and Methods
Figs. S1 to S25
Tables S1 to S11
References (41–77)

[9]Alamogordo Primate Facility, Holloman Air Force Base, New Mexico, USA

[10]Fishberg Department of Neuroscience and Friedman Brain Institute, Icahn School of Medicine at Mount Sinai, New York, New York, USA

[11]Lieber Institute for Brain Development, Johns Hopkins University Medical Campus, Baltimore, Maryland, USA

[12]Neuroscience Program, Michigan State University, East Lansing, Michigan, USA

[13]Department of Genetics, Yale School of Medicine, New Haven, Connecticut, USA

[14]Howard Hughes Medical Institute

[15]Yale Center for Genomic Analysis, Yale School of Medicine, New Haven, Connecticut, USA

[16]Department of Psychiatry and Langley Porter Psychiatric Institute, University of California, San Francisco, San Francisco, California, USA

[17]Allen Institute for Brain Science, Seattle, Washington, USA

[18]Department of Psychiatry and Zilkha Neurogenetic Institute, Keck School of Medicine, University of Southern California, Los Angeles, California, USA

[19]Institució Catalana de Recerca i Estudis Avançats, Barcelona, Catalonia, Spain

[20]Centro Nacional de Analisis Genomico, Barcelona, Catalonia, Spain

[21]Department of Anthropology, The George Washington University, Washington, District of Columbia, USA

[22]Program in Cellular Neuroscience, Neurodegeneration and Repair and Yale Child Study Center, Yale School of Medicine, New Haven, Connecticut, USA

Abstract

To better understand the molecular and cellular differences in brain organization between human and non-human primates, we performed transcriptome sequencing of sixteen regions of adult human, chimpanzee, and macaque brains. Integration with human single-cell transcriptomic data revealed global, regional, and cell-type specific species expression differences in genes representing distinct functional categories. We validated and further characterized the human specificity of genes enriched in distinct cell types through histological and functional analyses, including rare subpallial-derived interneurons expressing dopamine biosynthesis genes enriched in the human striatum and absent in the non-human African ape neocortex. Our integrated analysis of the generated data revealed diverse molecular and cellular features of the phylogenetic reorganization of the human brain across multiple levels of organization, with relevance for brain function and disease.

Introduction

Although the human brain is approximately three times larger than those of our closest living relatives, the non-human African great apes (chimpanzee, bonobo, and gorilla), increased size and neural cell counts fail to explain its unique functionalities (1–5). The

brain has also undergone microstructural, connectional, and molecular changes in the human lineage (1–5), changes likely mediated by divergent spatiotemporal gene expression (6–17).

Here, we profiled the mRNA and small noncoding RNA transcriptomes of sixteen adult brain regions involved in higher-order cognition and behavior of human (H, *Homo sapiens*), chimpanzee (C, *Pan troglodytes*) - our closest extant relative - and rhesus macaque (M, *Macaca mulatta*) - a commonly studied non-human primate. We integrated these profiles with single-cell transcriptomic data from the human brain (18, 19), histological data from adult and developmental brains of these and other primates (bonobo, gorilla, orangutan, pig-tailed macaque, baboon, and capuchin), and multimodal data from human primary and induced pluripotent stem cell (iPSC)-derived neural cultures. In doing so, we have investigated the evolutionary, cellular, and developmental framework that makes the human brain unique.

Overview of regional transcriptome profiling

We generated transcriptional profiles of 247 tissue samples representing hippocampus, amygdala, striatum, mediodorsal nucleus of thalamus, cerebellar cortex, and eleven areas of the neocortex from six humans, five chimpanzees, and five macaques (figs. S1–S5; table S1). To minimize biases in comparative transcriptome analyses, we used the *XSAnno* pipeline to create a common annotation set of 26,514 orthologous mRNAs, including 16,531 protein-coding genes and 3,253 long intergenic non-coding (linc) RNAs (fig. S2). We re-annotated all chimpanzee and macaque micro RNAs (miRNAs) based on annotated human precursor sequences (fig. S3). Assessment of global correlation between regions and species by unsupervised hierarchical clustering (fig. S5) revealed clustering of the miRNA dataset primarily by species. In contrast, cerebellar mRNA samples from all species formed a distinct cluster separated from other brain regions (fig. S5), indicating that the various cerebella are more similar to each other than to other brain regions within the same species. Within each species, hierarchical clustering of mRNA or miRNA datasets were calculated based on pairwise correlation matrices of brain regions and confirmed by multiscale bootstrap resampling and intra-species genetic distance measurements (figs. S6–7). This revealed a similar pattern of inter-regional hierarchical clustering, reflecting known topographical proximity and functional overlap (11, 14).

Species differences in regional gene expression

Differentially expressed genes were identified (False Discovery Rate [FDR] < 0.01) in each region by comparing generalized linear models with species as the main factor and batch as a cofactor. We found 25.9% of mRNAs (6,866 of 26,514) and 40.6% of miRNAs (603 of 1,485 mature miRNAs included in the analysis) were differentially expressed between at least two species in one or more regions. 11.9% of mRNAs (3,154) and 13.6% of miRNAs (202), representing distinct functional categories, exhibited human-specific upregulation (H>C=M) or downregulation (H<C=M; Figs. 1A–B; tables S2–4), with the highest number of differentially expressed genes observed in striatum followed by thalamus, primary visual cortex, and dorsolateral prefrontal cortex (fig. S8; table S3). These observations were not attributable to variations in the ratio of major cell types among species (fig. S9).

Among the 3,154 mRNA genes with human-specific differential expression, only 22 were upregulated and 9 down-regulated across all analyzed regions (fig. S10). Only 3 genes were differentially expressed across analyzed neocortical areas: *TWIST1* (down-regulated), a transcriptional regulator of neural genes that is mutated in Saethre–Chotzen syndrome, a disorder associated with intellectual disability (20) (Fig. 1C; fig. S11A–B), and two functionally uncharacterized lincRNAs (*RP11-364P22.1* and *CTB-78F1.1*; upregulated). The remaining 3,120 mRNA genes displayed human-specific differential expression in one or a subset of brain regions or neocortical areas (Fig. 1C; fig. S10; table S3). Among miRNAs, 10.4% (155) and 3.2% (47) were upregulated or downregulated, respectively, in the human brain with many displaying region-specific patterns (Fig. 1B; fig. S12). Independently validated examples include: *PKD2L1* (upregulated in neocortical areas except primary motor cortex), a gene encoding an ion channel (21); *MET* (upregulated in prefrontal cortex), a gene implicated in autism spectrum disorder (22); *ZP2* (upregulated in cerebellum), a gene encoding a protein mediating sperm-egg recognition (23); and several miRNAs (Fig. 1C; figs. S11–S12).

Species differences in gene co-expression patterns

To extract additional biologically relevant information, we applied weighted gene co-expression correlation network analysis (WGCNA) to generate modules of genes with similar variation across regions and/or species. We identified 229 mRNA modules, many of which exhibited regional and/or species-specific expression patterns (Figs. 2A–B; table S5). For example, genes in module 92 (M92) and M32 are respectively upregulated and downregulated in human neocortex, and M130 genes are upregulated in human striatum, hippocampus, and amygdala (fig. S13). M130 includes tyrosine hydroxylase (*TH*) and DOPA decarboxylase (*DDC*), both involved in dopamine biosynthesis (fig. S13F). Human-specific modules were enriched for genes associated with categories and pathways such as “Thrombospondin N-terminal-like domains” and “alternative splicing” (table S5).

We also clustered all miRNAs based on their individual correlations to the average expression profile of each mRNA module (fig. S14A; table S6). Because the expression of each miRNA might correlate with multiple mRNA modules, module pairings were refined using a transcriptome-wide HITS-CLIP map of miRNA binding sites in the human brain (24) (fig. S14B; table S7). We identified 37 stable miRNA modules, with several pairs of miRNA/mRNA modules exhibiting opposing regional and/or species-specific enrichment for potential miRNA-mRNA target predictions (fig. S14C–E).

Cell-type specificity of differentially expressed genes

To investigate differential gene expression patterns at the cellular level, we integrated our datasets with single-cell RNA-seq data generated from the human neocortex (18, 19) and validated findings via immunohistochemistry or *in situ* hybridization. We found that many of the genes displaying species- and/or region-specific patterns also exhibited cell-type specific expression. For example, *PKD2L1* is enriched in excitatory projection neurons (Figs. 3A and 3C), *TH* is expressed in a subset of somatostatin (*SST*)-expressing inhibitory interneurons in human and macaque neocortical deep layers and white matter (Figs. 3B and 3D), and *ZP2* is

upregulated in the granule cells of the human cerebellum (figs. S11C–D). Additionally, we found cell-type specific enrichment among WGCNA modules, including human-specific M81 and M162, which were composed of genes enriched in a subset of neocortical excitatory projection neurons (Fig. 2B, right panels; table S5).

Species differences in neurotransmitter receptor gene expression

The species- and region-specific expression patterns of several genes associated with neurotransmission prompted us to investigate whether there were broad inter-species differences in the co-expression networks and genomic sequences of genes encoding receptors underlying excitatory, inhibitory, or modulatory signaling (figs. S15A–D). Gene co-expression networks of the cholinergic and serotonergic systems differed among the three species (figs. S15E–F). While the dopaminergic system did not have enough genes for reliable network construction, we found that *DRD1*, *DRD2*, and *DRD3*, genes encoding dopamine receptors, exhibited human-specific downregulation in striatum (fig. S10). By contrast, excitatory glutamatergic and inhibitory GABAergic systems' genes exhibited conserved networks among species and their coding sequences were more conserved than the coding sequences of genes with similar expression levels (figs. S15–17; table S8).

Species differences in dopamine biosynthesis gene expression

We next investigated dopamine biosynthesis and signaling genes. *TH* and *DDC* displayed human-specific (H>C=M) upregulation in the striatum (Fig. 4A). *TH* also displayed chimpanzee-specific downregulation (C<H=M) in the neocortex (Fig. 4A). An extended analysis of RNA-seq data (25) independently validated the downregulation of *TH* mRNA in chimpanzee neocortex compared to human, as well as the downregulation of *TH* expression in the neocortex of bonobo and gorilla, but not of orangutan (fig. S18A).

Analyses of *cis*-regulatory elements active near the *TH* gene in the adult human, chimpanzee, and macaque brain (26) revealed no differences that would explain observed *TH* expression patterns. We hypothesized that the species-specific *TH* expression patterns might be explained by changes in the number and distribution of TH-expressing interneurons, which have been previously identified in telencephalic regions and shown to vary in distribution across species (27–29), including depletion in the prefrontal cortex of non-human great apes (28). Therefore, we quantified TH-immunopositive (TH+) interneurons (figs. S19A–C) on an independent set of 45 adult brains from 9 primate species (table S9). Consistent with our transcriptome data, humans have a higher number (Tukey's honest significance test all $P < 0.05$) of TH+ interneurons in both the dorsal caudate nucleus and putamen (striatum) when compared to all other analyzed non-human primates (Fig. 4C; fig. S20A). Furthermore, we found neocortical TH+ interneurons in all analyzed areas of human, all monkey species, and orangutan (Fig. 4C, figs. S20B; S20D), but only TH+ fibers in all analyzed neocortical areas of chimpanzee, bonobo, and gorilla (Fig. 4C; fig. S20B). We found no differences in the number of TH+ interneurons in human, chimpanzee, gorilla, and macaque olfactory bulbs (fig. S19D).

Molecular profiling of human TH+ interneurons

To further explore the phenotype of adult human neocortical TH+ interneurons, we performed immunohistochemistry and *in situ* hybridization. TH+ interneurons expressed GAD1, the GABA synthesis enzyme (Fig. 4B), but were lacking canonical markers of neocortical interneuron subtypes such as SST, PVALB, NPY, NOS1, CALB2, and VIP (fig. S21), as well as *ETV1*, which is required for differentiation of dopaminergic neurons in multiple species (30), or its homolog, *ETV5* (figs. S21H–I). Most TH+/GAD1+ interneurons co-expressed DDC (62.54 ± 1.01%; Fig. 4B), the enzyme that converts L-DOPA to dopamine, but not DBH (fig. S18; 31), the enzyme that converts dopamine to noradrenaline, indicating that a subset of TH+ interneurons are able to produce dopamine, but not noradrenaline.

Developmental origin of human TH+ interneurons

To gain insight into the development of TH+ interneurons, we analyzed the regional expression of *TH* across human brain development using the BrainSpan RNA-seq dataset (www.brainspan.org). The highest *TH* expression is observed in striatum and increases steadily from early fetal development (period 2, as defined in ref. 11) to young adulthood (period 13; Fig. 5A). Lower *TH* expression is observed in neocortex, hippocampus, and amygdala and increases perinatally (periods 7 [late fetal development] and 8 [early infancy]) and remains stable in neocortex. In addition, *TH* expression increases from early childhood (period 10) to young adulthood in the amygdala and hippocampus (Fig. 5A).

Using immunohistochemistry, we detected TH+ axons in striatum as early as late midfetal development (fig. S22), and occasional bipolar TH+ interneurons were first observed in the external capsule and neocortical white matter in the newborn human (Fig. 5B). The neonatal chimpanzee brain displayed the same pattern of unmyelinated TH+ fibers in the external capsule (Fig. 5B), but no TH+ interneurons were detected in the neocortex.

To identify the birthplace of TH+ interneurons, we prepared primary cell cultures from 17–18 postconceptional week (pcw)-old human brains (Fig. 5C) of lateral, medial, and caudal ganglionic eminences (LGE, MGE, and CGE) of the ventral forebrain (subpallium), known to generate interneurons (32–34), and neocortical proliferative zones, which may also generate interneurons in humans (13). We found TH+ interneurons co-expressing canonical markers of distinct progenitor lineages within ganglionic eminences (NKX2-1, NR2F2, or SP8) (Fig. 5D). BrdU birthdating confirmed that TH+ interneurons are generated by ganglionic eminence, but not neocortical, progenitors (Fig. 5D–E), indicating that TH+ interneurons are derived from diverse subpallial lineages and are developmentally heterogeneous. Similar to adult neocortical TH+ interneurons, subpallial-derived TH+ interneurons also co-expressed GAD1 and DDC (Fig. 5D). Neocortical TH+ interneurons were mainly SP8+ (77.68 ± 12.11%), with a smaller NR2F2+ (22.22 ± 8.78%) subpopulation, and were all BrdU−, indicating that they began to migrate into neocortex before 17 pcw, but express TH protein later in development (Fig. 5D–E).

In vitro characterization of human TH+ interneurons

To further characterize TH+ interneuron development and properties, we asked whether TH + interneurons could be generated from human iPSCs using a differentiation protocol for cortical excitatory projection neurons and inhibitory interneurons (fig. S23; Methods). Immunofluorescence confirmed the presence of TH+ cells co-expressing GAD1 and SP8, but not SST, PVALB, NR2F2, or NKX2-1, confirming that iPSC-derived TH+ interneurons display a similar molecular profile to TH+ interneurons from the adult neocortex and neocortical primary culture (fig. S24). Complementary analysis of a single-cell RNA-seq dataset from human embryonic stem cell-derived cortical interneurons (35) revealed that many *TH*-expressing cells co-express GABAergic marker genes *GAD1/2* at all time points, as well as *SST*, *ETV1,* and *ETV5* transiently at early time points (fig. S25).

We characterized human iPSC-derived TH+ interneurons by assessing their ability to produce and transport dopamine using immunofluorescence, a monoamine uptake assay, and high-performance liquid chromatography. We found that 72.1 ± 10.0% of 80 DIV TH+ interneurons that had taken up a monoamine-imitating fluorophore were DDC+ (Fig. 6A–B), and consequently could produce and transport dopamine *in vitro*. Commensurate with these observations, we detected dopamine in conditioned culture media from iPSC-derived and LGE primary neural cultures, both of which contained TH+/DDC+ interneurons, but not in control culture media (Fig. 6C).

Discussion

Our analysis of transcriptomic data revealed global, regional, and cell-type specific species expression differences in protein-coding and non-coding genes. Genes with human-specific differential expression patterns include those encoding transcription factors, ion channels, and neurotransmitter biosynthesis enzymes and receptors. Changes in the regional and cellular expression patterns of these genes could affect function of neural circuits by altering transcription of other genes, intrinsic electrophysiological properties, or synaptic transmission.

Neuromodulatory systems show broad expression differences between species. One example includes a rare and molecularly heterogeneous subpopulation of interneurons expressing dopamine biosynthesis genes *TH* and *DDC*, which are enriched in the human striatum and neocortex as compared to non-human African apes. These cells originate in the subpallial ganglionic eminences and likely migrate into the striatum and neocortex during late prenatal and early postnatal development. We also observed an increase in *TH* expression during postnatal development and young adulthood, suggesting that *TH* expression and/or the migration of TH+ interneurons may be dynamically regulated and protracted.

The absence of TH+ interneurons from the cortex of non-human African apes (see also 28), and their decreased density in the striatum of non-human primates, may result from several mechanisms. First, these cells could have been lost due to genetic disruptions affecting interneuron migration, differentiation, or survival (32–34). These disruptions may have occurred in the common ancestor of African apes prior to being reversed in the human

lineage (homoplasy) or, in a less-likely scenario, may have occurred independently in the Gorilla and Pan lineages. A second possibility is that these interneurons are present in the non-human African ape cortex but do not express TH, do so only transiently, or die prior to our ability to detect them. Commensurate with this possibility, the molecular profile of mouse cortical SST-positive interneurons is malleable (36) and sensory stimuli can cause a switch from the production of TH and dopamine to SST in rat hypothalamic interneurons (37). Finally, TH+ interneurons of non-human African apes may have lost their ability to deviate to cortex from the rostral migratory stream. Indeed some human TH+ interneurons migrating via the rostral migratory stream to the olfactory bulb divert to the prefrontal cortex (38) and our observation of SP8+/TH+ co-expression is consistent with a rostral migratory stream origin. However, other routes of migration are possible, as suggested by our observation of TH+ interneurons in the external capsule of newborn human brain.

Neuromodulatory transmitters, in particular dopamine, are involved in distinctly human aspects of cognition and behavior, such as working memory, reasoning, reflective exploratory behavior, and overall intelligence. By analyzing brain regions involved in these processes, we show that evolutionary modifications in gene expression and the distribution of neurons associated with neuromodulatory systems may underlie cognitive and behavioral differences between species. Cortical TH+ interneurons are depleted in patients affected by Parkinson’s disease (39) or dementia with Lewy bodies (40), and these alterations may contribute to cognitive impairments.

As these results demonstrate, the resource we present here may aid future studies on the evolution and neuroscience of primates.

Supplementary Material

Refer to Web version on PubMed Central for supplementary material.

Acknowledgments

We thank A. Bauernfeind, M. Horn, D. Singh, G. Terwilliger, I.B. Toxopeus, B. Wicinski, and S. Wilson for assistance with tissue acquisition and processing, and the Alamogordo Primate Facility and the Primate Brain Bank, Netherlands Institute for Neuroscience, for providing primate tissue. Data was generated as part of the PsychENCODE Consortium, supported by MH103339, MH106934, and MH110926. Additional support was provided by the NIH grant MH109904, the Kavli Foundation, the James S. McDonnell Foundation, NSF grant BCS-1316829, and ERC Starting Grant 260372, and MICINN BFU2011-28549. Supplement contains additional data.

References

1. Preuss, TM. What is it like to be a human. In: Gazzaniga, MS., editor. The Cognitive Neurosciences. MIT Press; Cambridge, MA: 2004. p. 5-22.
2. Sherwood CC, Subiaul F, Zawidzki TW. A natural history of the human mind: tracing evolutionary changes in brain and cognition. J. Anat. 2008; 212:426–454. [PubMed: 18380864]
3. Teffer K, Semendeferi K. Human prefrontal cortex: evolution, development, and pathology. Prog. Brain Res. 2012; 195:191–218. [PubMed: 22230628]
4. Gabi M, et al. No relative expansion of the number of prefrontal neurons in primate and human evolution. Proc. Nat.l Aca.d Sci. U.S.A. 2016; 113:9617–9622.

5. Sousa AMM, Meyer KA, Santpere G, Gulden FO, Sestan N. Evolution of the human nervous system function, structure, and development. Cell. 2017; 170:226–247. [PubMed: 28708995]
6. King MC, Wilson AC. Evolution at two levels in humans and chimpanzees. Science. 1975; 188:107–116. [PubMed: 1090005]
7. Cáceres M, et al. Elevated gene expression levels distinguish human from non-human primate brains. Proc. Natl. Acad. Sci. U.S.A. 2003; 100:13030–13035. [PubMed: 14557539]
8. Uddin M, et al. Sister grouping of chimpanzees and humans as revealed by genome-wide phylogenetic analysis of brain gene expression profiles. Proc. Natl. Acad. Sci. U.S.A. 2004; 101:2957–2962. [PubMed: 14976249]
9. Khaitovich P, et al. Parallel patterns of evolution in the genomes and transcriptomes of humans and chimpanzees. Science. 2005; 309:1850–1854. [PubMed: 16141373]
10. Babbitt CC, et al. Both noncoding and protein-coding RNAs contribute to gene expression evolution in the primate brain. Genome Biol. Evol. 2010; 2:67–79. [PubMed: 20333225]
11. Kang HJ, et al. Spatio-temporal transcriptome of the human brain. Nature. 2011; 478:483–489. [PubMed: 22031440]
12. Konopka G, et al. Human-specific transcriptional networks in the brain. Neuron. 2012; 75:601–617. [PubMed: 22920253]
13. Geschwind DH, Rakic P. Cortical evolution: judge the brain by its cover. Neuron. 2013; 80:633–647. [PubMed: 24183016]
14. Pletikos M, et al. Temporal specification and bilaterality of human neocortical topographic gene expression. Neuron. 2014; 81:321–332. [PubMed: 24373884]
15. Bae BI, Jayaraman D, Walsh CA. Genetic changes shaping the human brain. Dev. Cell. 2015; 32:423–434. [PubMed: 25710529]
16. Silver DL. Genomic divergence and brain evolution: how regulatory DNA influences development of the cerebral cortex. Bioessays. 2016; 38:162–171. [PubMed: 26642006]
17. Lein ES, Belgard TG, Hawrylycz M, Molnar Z. Transcriptomic perspectives on neocortical structure, development, evolution, and disease. Annu. Rev. Neurosci. 2017; 40:629–652. [PubMed: 28661727]
18. Darmanis S, et al. A survey of human brain transcriptome diversity at the single cell level. Proc. Natl. Acad. Sci. U.S.A. 2015; 112:7285–7290. [PubMed: 26060301]
19. Lake BB, et al. Neuronal subtypes and diversity revealed by single-nucleus RNA sequencing of the human brain. Science. 2016; 352:1586–1590. [PubMed: 27339989]
20. Howard TD, et al. Mutations in TWIST, a basic helix-loop-helix transcription factor, in Saethre-Chotzen syndrome. Nat. Genet. 1997; 15:36–41. [PubMed: 8988166]
21. Huang AL, et al. The cells and logic for mammalian sour taste detection. Nature. 2006; 442:934–938. [PubMed: 16929298]
22. Campbell DB, et al. A genetic variant that disrupts MET transcription is associated with autism. Proc. Natl. Acad. Sci. U.S.A. 2006; 103:16834–16839. [PubMed: 17053076]
23. Hoodbhoy T, Dean J. Insights into the molecular basis of sperm-egg recognition in mammals. Reproduction. 2004; 127:417–422. [PubMed: 15047932]
24. Boudreau RL, et al. Transcriptome-wide discovery of microRNA binding sites in human brain. Neuron. 2014; 81:294–305. [PubMed: 24389009]
25. Brawand D, et al. The evolution of gene expression levels in mammalian organs. Nature. 2011; 478:343–348. [PubMed: 22012392]
26. Vermunt MW, et al. Epigenomic annotation of gene regulatory alterations during evolution of the primate brain. Nat. Neurosci. 2016; 19:494–503. [PubMed: 26807951]
27. Berger B, Verney C, Gaspar P, Febvret A. Transient expression of tyrosine hydroxylase immunoreactivity in some neurons of the rat neocortex during postnatal development. Brain Res. 1985; 355:141–144. [PubMed: 2866813]
28. Raghanti MA, et al. Species-specific distributions of tyrosine hydroxylase-immunoreactive neurons in the prefrontal cortex of anthropoid primates. Neuroscience. 2009; 158:1551–1559. [PubMed: 19041377]

29. Benavides-Piccione R, DeFelipe J. Distribution of neurons expressing tyrosine hydroxylase in the human cerebral cortex. J. Anat. 2007; 211:212–222. [PubMed: 17593221]
30. Flames N, Hobert O. Gene regulatory logic of dopamine neuron differentiation. Nature. 2009; 458:885–889. [PubMed: 19287374]
31. Gaspar P, Berger B, Febvret A, Vigny A, Henry JP. Catecholamine innervation of the human cerebral-cortex as revealed by comparative immunohistochemistry of tyrosine-hydroxylase and dopamine-beta-hydroxylase. J. Comp. Neurol. 1989; 279:249–271. [PubMed: 2563268]
32. Hansen DV, Lui JH, Parker PRL, Kriegstein AR. Neurogenic radial glia in the outer subventricular zone of human neocortex. Nature. 2010; 464:554–561. [PubMed: 20154730]
33. Ma T, et al. Subcortical origins of human and monkey neocortical interneurons. Nat. Neurosci. 2013; 16:1588–1597. [PubMed: 24097041]
34. Kepecs A, Fishell G. Interneuron cell types are fit to function. Nature. 2014; 505:318–326. [PubMed: 24429630]
35. Close JL, et al. Single-cell profiling of an in vitro model of human interneuron development reveals temporal dynamics of cell type production and maturation. Neuron. 2017; 93:1035–1048. [PubMed: 28279351]
36. Dehorter N, et al. Tuning of fast-spiking interneuron properties by an activity-dependent transcriptional switch. Science. 2015; 349:1216–1220. [PubMed: 26359400]
37. Dulcis D, Jamshidi P, Leutgeb S, Spitzer NC. Neurotransmitter switching in the adult brain regulates behavior. Science. 2013; 340:449–453. [PubMed: 23620046]
38. Sanai N, et al. Corridors of migrating neurons in the human brain and their decline during infancy. Nature. 2011; 478:382–386. [PubMed: 21964341]
39. Fukuda T, Takahashi J, Tanaka J. Tyrosine hydroxylase-immunoreactive neurons are decreased in number in the cerebral cortex of Parkinson's disease. Neuropathology. 1999; 19:10–13. [PubMed: 19519642]
40. Marui W, Iseki E, Kato M, Kosaka K. Degeneration of tyrosine hydroxylase-immunoreactive neurons in the cerebral cortex and hippocampus of patients with dementia with Lewy bodies. Neurosci. Lett. 2003; 340:185–188. [PubMed: 12672537]
41. USDA. 7 USC, Title 7-AGRICULTURE. CHAPTER 54 - TRANSPORTATION, SALE, AND HANDLING OF CERTAIN ANIMALS. Washington, D.C.: U.S. Goverment Printing Office; 2013. Animal Welfare Act and Animal Welfare Regulations. http://awic.nal.usda.gov/government-and-professional-resources/federal-laws/animal-welfare-act
42. NIH/OLAW. U.S. Government Principles for the Utilization and Care of Vertebrate Animals Used in Testing, Research, and Training. 2002. http://grants.nih.gov/grants/olaw/references/phspol.htm#PublicHealthServicePolicyonHumaneCareandUseofLaboratory
43. National Research Council. Guide for the Care and Use of Laboratory Animals. 8. The National Academies Press; 2011.
44. DeLucchi, MR., Dennis, BJ., Adey, WR. A stereotaxic atlas of the chimpanzee brain (Pan satyrus). University of California Press; Berkeley and Los Angeles: 1965.
45. Saleem, KS., Logothetis, N. A combined MRI and histology atlas of the rhesus monkey brain in stereotaxic coordinates. Academic Press; San Diego: 2007.
46. Jiang L, et al. Synthetic spike-in standards for RNA-seq experiments. Genome Res. 2011; 22:1543–1551.
47. Trapnell C, Pachter L, Salzberg SL. TopHat: discovering splice junctions with RNA-Seq. Bioinformatics. 2009; 25:1105–1111. [PubMed: 19289445]
48. Zhu Y, Li M, Sousa AMM, Sestan N. XSAnno: A framework for annotating orthologs in cross-species transcriptome comparisons. BMC Genomics. 2014; 15:343. [PubMed: 24884593]
49. Harrow J, et al. GENCODE: the reference human genome annotation for The ENCODE Project. Genome Res. 2012; 22:1760–1774. [PubMed: 22955987]
50. Hinrichs AS, et al. The UCSC Genome Browser Database: update 2006. Nucl. Acids Res. 2006; 34:D590–D598. [PubMed: 16381938]
51. Habegger L, et al. RSEQtools: a modular framework to analyze RNA-Seq data using compact, anonymized data summaries. Bioinformatics. 2011; 27:281–283. [PubMed: 21134889]

52. Mortazavi A, Williams BA, McCue K, Schaeffer L, Wold B. Mapping and quantifying mammalian transcriptomes by RNA-Seq. Nature Meth. 2008; 5:621–628.
53. Team, RC. R: A language and environment for statistical computing. R Foundation for Statistical Computing; 2013.
54. Johnson WE, Li C, Rabinovic A. Adjusting batch effects in microarray expression data using empirical Bayes methods. Biostatistics. 2007; 8:118–127. [PubMed: 16632515]
55. Zhang Y, et al. Purification and characterization of progenitor and mature human astrocytes reveals transcriptional and functional differences with mouse. Neuron. 2016; 89:37–53. [PubMed: 26687838]
56. Anders S, Huber W. Differential expression analysis for sequence count data. Genome Biol. 2010; 11:R106. [PubMed: 20979621]
57. Suzuki R, Shimodaira H. Pvclust: an R package for assessing the uncertainty in hierarchical clustering. Bioinformatics. 2006; 22:1540–1542. [PubMed: 16595560]
58. Langfelder P, Horvath S. WGCNA: an R package for weighted correlation network analysis. BMC Bioinformatics. 2008; 9:559. [PubMed: 19114008]
59. Zhang B, Horvath S. A general framework for weighted gene co-expression network analysis. Stat. Applic. Gen. Mol. Biol. 2005; 4 Article17.
60. Langfelder P, Luo R, Oldham MC, Horvath S. Is my network module preserved and reproducible? PLoS Comput. Biol. 2011; 7:e1001057. [PubMed: 21283776]
61. Cunningham F, et al. Ensembl 2015. Nucl. Acids Res. 2015; 43:D662–669. [PubMed: 25352552]
62. Smedley D, et al. The BioMart community portal: an innovative alternative to large, centralized data repositories. Nucl. Acids Res. 2015; 43:W589–598. [PubMed: 25897122]
63. Baev V, Daskalova E, Minkov I. Computational identification of novel microRNA homologs in the chimpanzee genome. Comput. Biol. Chem. 2009; 33:62–70. [PubMed: 18760970]
64. Yue J, Sheng Y, Orwig KE. Identification of novel homologous microRNA genes in the rhesus macaque genome. BMC Genomics. 2008; 9:8. [PubMed: 18186931]
65. Hu HY, et al. MicroRNA expression and regulation in human, chimpanzee, and macaque brains. PLoS Genet. 2011; 7:e1002327. [PubMed: 22022286]
66. Langmead B, Trapnell C, Pop M, Salzberg SL. Ultrafast and memory-efficient alignment of short DNA sequences to the human genome. Genome Biol. 2009; 10:R25. [PubMed: 19261174]
67. Hackenberg M, Rodríguez-Ezpeleta N, Aransay AM. miRanalyzer: an update on the detection and analysis of microRNAs in high-throughput sequencing experiments. Nucl. Acids Res. 2011; 39:W132–W138. [PubMed: 21515631]
68. Hofacker IL. Vienna RNA secondary structure server. Nucl. Acids Res. 2003; 31:3429–3431. [PubMed: 12824340]
69. Gentleman RC, et al. Bioconductor: open software development for computational biology and bioinformatics. Genome Biol. 2004; 5:R80. [PubMed: 15461798]
70. Li H, et al. The Sequence Alignment/Map format and SAMtools. Bioinformatics. 2009; 25:2078–2079. [PubMed: 19505943]
71. Purcell S, et al. PLINK: a tool set for whole-genome association and population-based linkage analyses. Am. J. Hum. Genet. 2007; 81:559–575. [PubMed: 17701901]
72. Tamura K, et al. MEGA5: molecular evolutionary genetics analysis using maximum likelihood, evolutionary distance, and maximum parsimony methods. Mol. Biol. Evol. 2011; 28:2731–2739. [PubMed: 21546353]
73. Okita K, et al. An Efficient Nonviral Method to Generate Integration-Free Human-Induced Pluripotent Stem Cells from Cord Blood and Peripheral Blood Cells. Stem Cells. 2013; 31:458–466. [PubMed: 23193063]
74. Chambers SM, et al. Highly efficient neural conversion of human ES and iPS cells by dual inhibition of SMAD signaling. Nature Biotechnol. 2009; 27:275–280. [PubMed: 19252484]
75. Onorati M, et al. Molecular and functional definition of the developing human striatum. Nat. Neurosci. 2014; 17:1804–1815. [PubMed: 25383901]
76. Stutz B, et al. Murine dopaminergic Müller cells restore motor function in a model of Parkinson's disease. J. Neurochem. 2014; 128:829–840. [PubMed: 24117434]

77. Prado-Martinez J, et al. Great ape genetic diversity and population history. Nature. 2013; 499:471–475. [PubMed: 23823723]

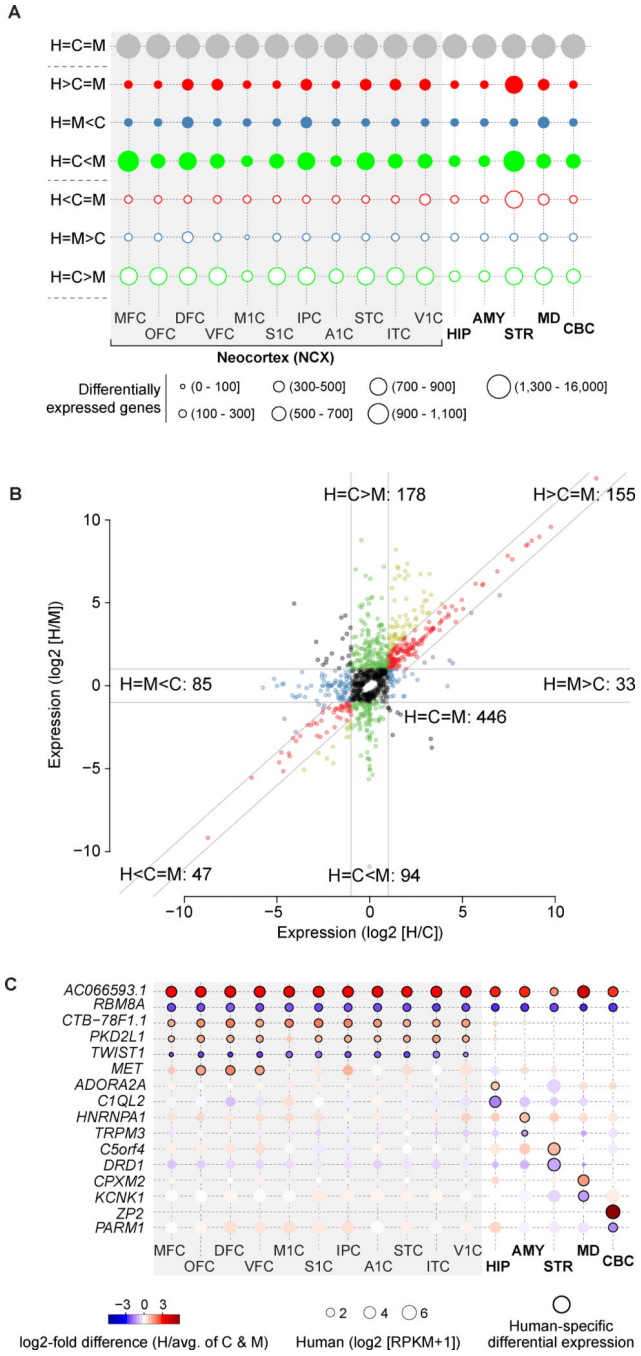

Fig. 1. Inter-species differential gene expression across sixteen brain regions

(**A**) Bubble matrix showing the number of mRNA genes with conserved expression (grey circles), species-specific upregulation (filled circles), or downregulation (open circles). Post-hoc comparisons described in table S2. H – human; C – chimpanzee; M – macaque. (**B**) Inter-species patterns of normalized miRNA expression across all regions. Guidelines indicate ± 2-fold difference. (**C**) Examples of protein-coding and non-coding genes exhibiting global and regional human-specific upregulation (red and circles with black borders) or downregulation (blue and circles with black borders). Additional information

and validations are provided in figs. S10–S12. OFC – orbital prefrontal cortex; DFC – dorsolateral prefrontal cortex; VFC – ventrolateral prefrontal cortex; MFC – medial prefrontal cortex; M1C – primary motor cortex; S1C – primary somatosensory cortex; IPC – inferior posterior parietal cortex; A1C – primary auditory cortex; STC – superior temporal cortex; ITC – inferior temporal cortex; V1C – primary visual cortex; HIP – hippocampus; AMY – amygdala; STR – striatum; MD – mediodorsal nucleus of the thalamus; CBC – cerebellar cortex.

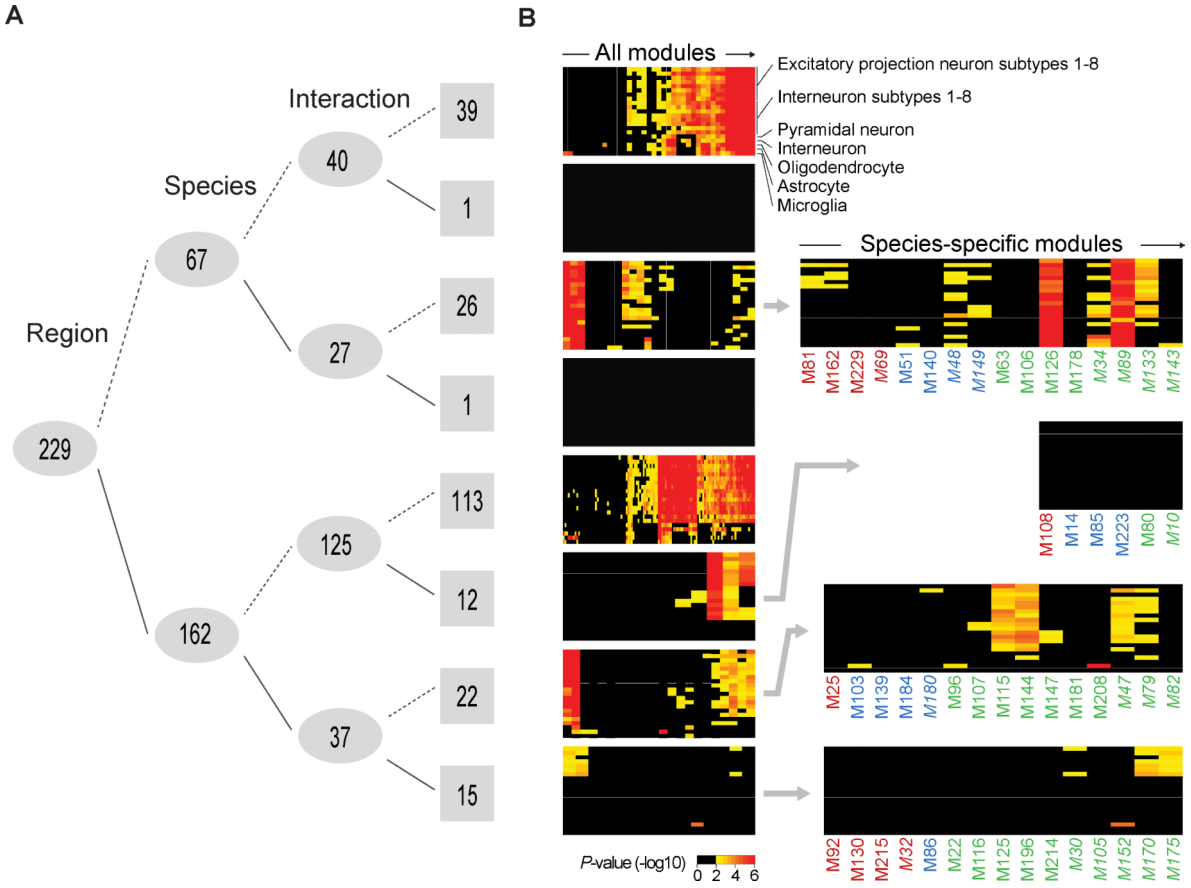

Fig. 2. Conserved and species-specific gene co-expression modules

(**A**) Number of WGCNA modules (numbers on grey; see table S5) clustered by differential expression across brain regions, species, and inter-species differences across regions (interaction) (ANOVA of eigengene Bonferroni adjusted $P < 0.01$, solid line; ≥ 0.01, dashed line). (**B**) Left panel: Enrichment of gene expression for modules (columns) in several cell types (rows) based on human single-cell transcriptome data (18, 19), sorted by unsupervised hierarchical clustering to show similarities among modules. Right panel: Species-specific modules showing human (red), chimpanzee (blue), or macaque (green) upregulation (normal font) or downregulation (italics) relative to the other two species exhibit distinct patterns of cell-type associated gene expression.

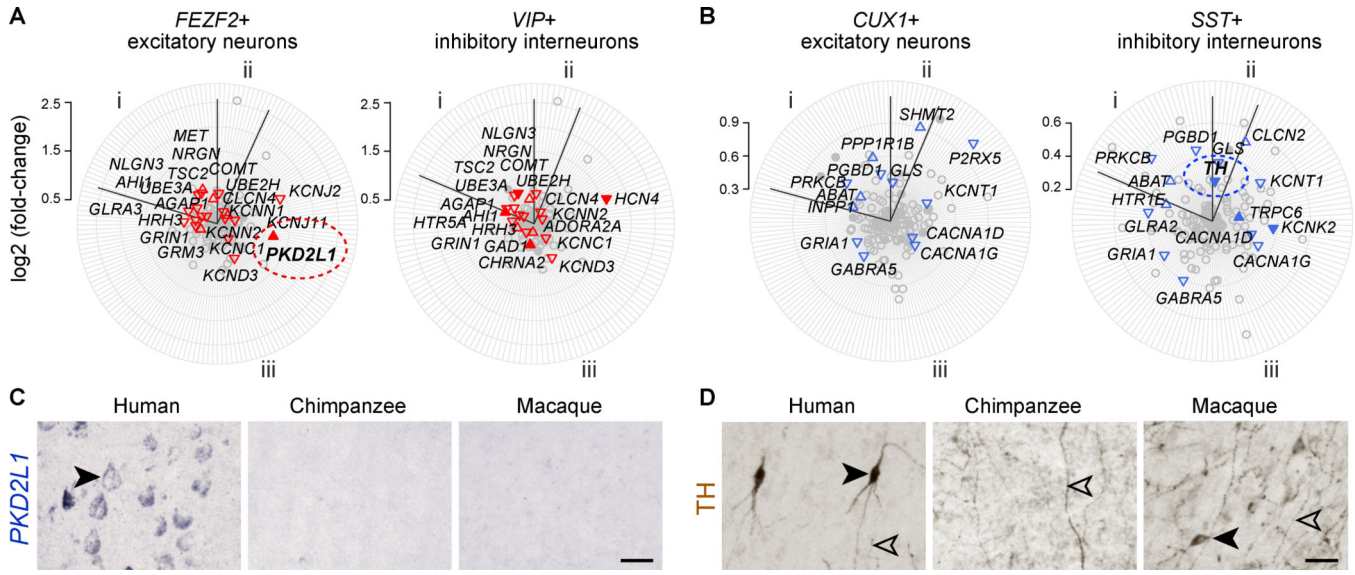

Fig. 3. Cellular specificity of neocortical human and chimpanzee-specific differential expression

(A–B) Radar plots depicting neocortical neuron cell-type enrichments of **(A)** human- or **(B)** chimpanzee-specific differences of genes associated with (i) neuropsychiatric disorders, (ii) neurotransmitter biosynthesis, degradation, and transport proteins, and (iii) encoding ion channels (table S10). Only genes expressed in the respective cell type are plotted. The distance of each gene from the center represents differential expression between human and the average of chimpanzee and macaque (red) or between chimpanzee and the other two species (blue). The direction of triangles denotes up- or downregulation; filled triangles represent cell-type specific expression (Pearson correlations > 0.5). **(C)** *In situ* hybridization shows that *PKD2L1* is expressed in pyramid-shaped cell bodies of excitatory projection neurons of human, but not chimpanzee or macaque, neocortex. **(D)** TH-immunopositive interneurons (filled arrowheads) are present in neocortex of human and macaque, but not chimpanzee, where only TH+ midbrain dopaminergic axons (open arrowheads) are present. Scale bar represents 30 μm.

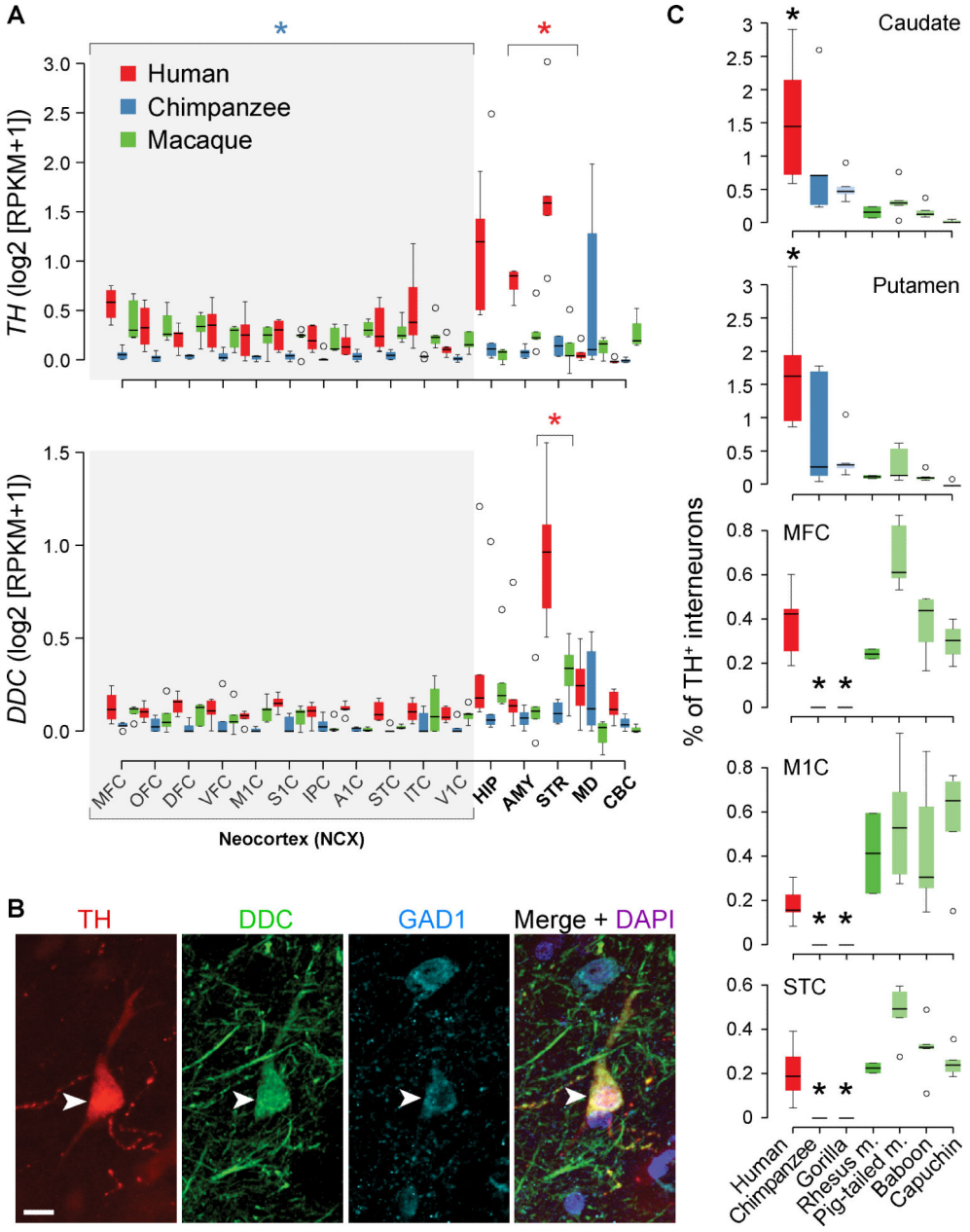

Fig. 4. Human-specific expression of genes encoding dopamine biosynthesis enzymes

(**A**) *TH* and *DDC*, respectively, showing higher expression in the human striatum (STR). *TH* is also downregulated in the chimpanzee neocortex. Boxes represent quartiles and whiskers 1.5 times interquartile range. Red and blue asterisks represent human-specific differential expression in striatum and chimpanzee-specific differential expression combining all neocortical areas, respectively (FDR < 0.01). (**B**) Immunofluorescence shows co-localization of TH, DDC, and GAD1 in adult human neocortical interneurons (arrowheads). Scale bar represents 10 μm. (**C**) STR (caudate and putamen) shows an enrichment of TH+ interneurons in human. MFC, M1C, and STC show a complete depletion of TH+ interneurons in chimpanzee and gorilla. Asterisk represents Tukey's honest significance test $P < 0.05$ comparing human or chimpanzee/gorilla with all other species.

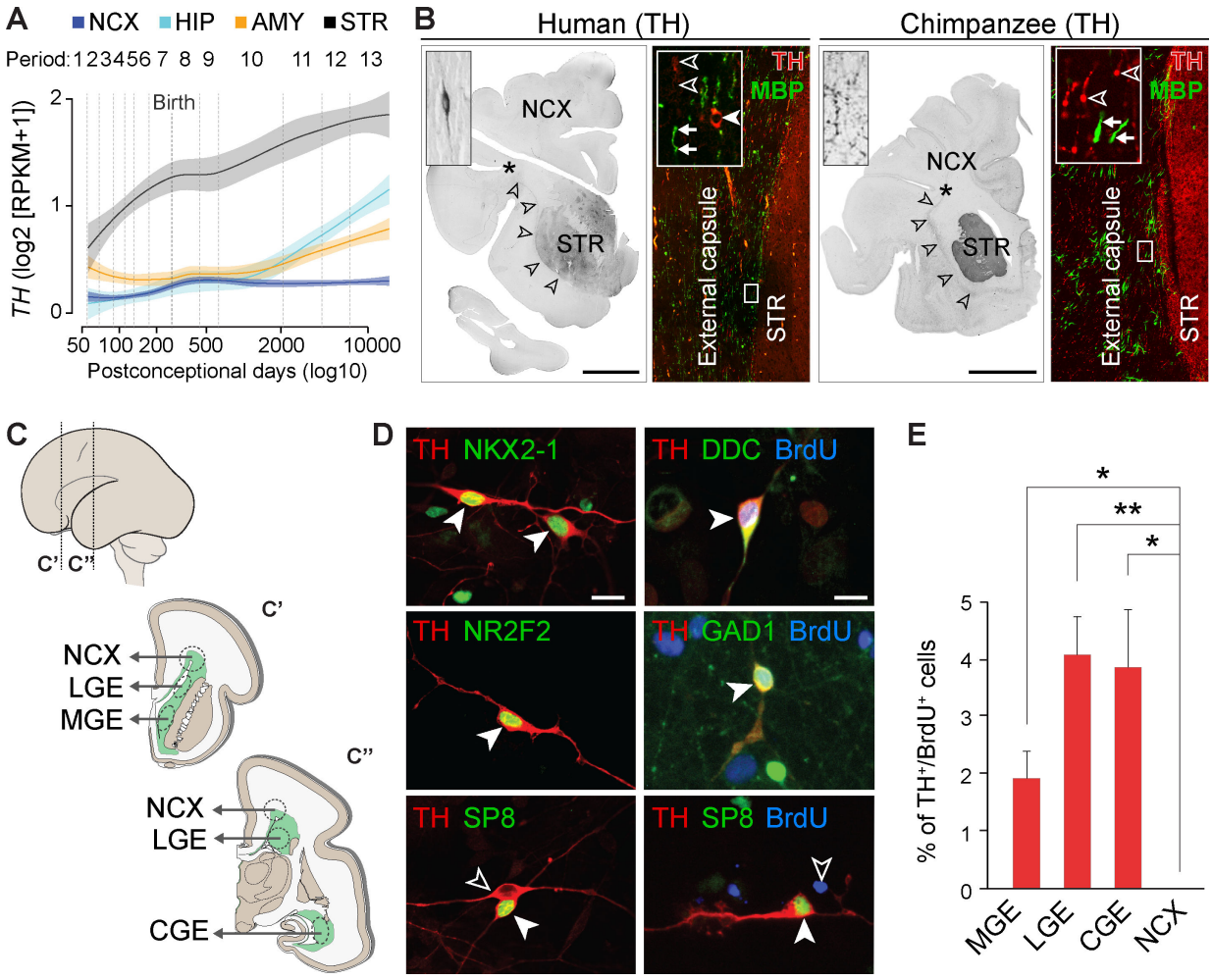

Fig. 5. Human telencephalic TH+ interneurons are of subpallial origin and start to express TH protein perinatally

(A) *TH* expression in human neocortex (NCX), HIP, AMY, and STR throughout development. The shaded area corresponds to a confidence interval of 50%. (**B**) Immunohistochemistry reveals TH+ axons in external capsule (arrowheads), STR, and NCX of newborn (38 pcw) human and chimpanzee brains. Bipolar TH+ interneurons (filled arrowhead) are present in parallel with MBP+/TH− (arrows) and TH+/MBP− (open arrowheads) fibers in the external capsule. No TH+ cells were detected in chimpanzee external capsule. Scale bar represents 1 cm. (**C**) Schematic of dissection of ganglionic eminences (lateral [LGE], medial [MGE], and caudal [CGE]) and neocortical proliferative zones (NCX) from mid-fetal brain for primary cell culture. (**D**) TH+ cells from ganglionic eminences also express NKX2-1, NR2F2, or SP8, and were BrdU+, DDC+, and GAD1+. TH+ interneurons in the neocortical culture were SP8+, but BrdU− (bottom right panel). Scale bar represents 20 μm. (**E**) Percentage of TH+/BrdU+ cells in culture from MGE, LGE, CGE, and NCX. Error bars represent SEM. Pairwise t-tests were performed and corrected for multiple testing using Bonferroni correction. * $P < 0.05$; ** $P < 0.01$.

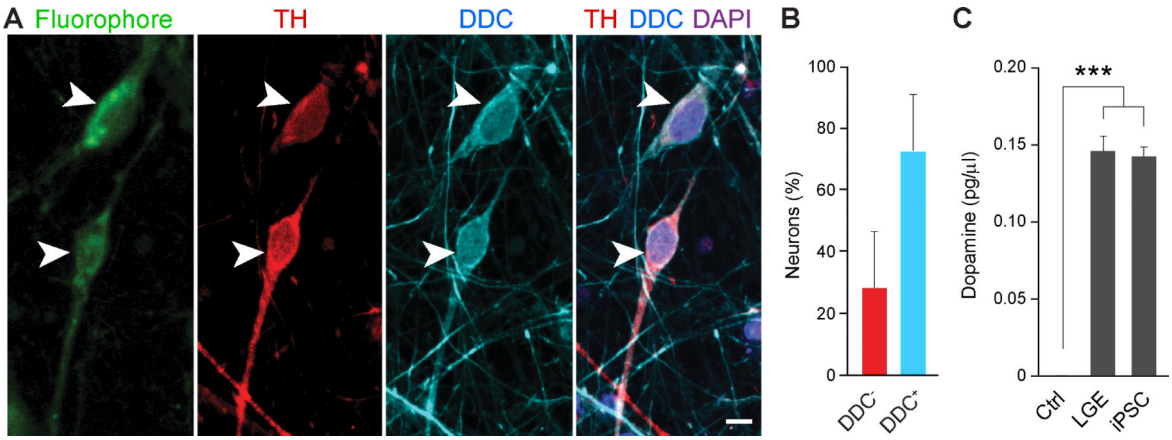

Fig. 6. Human telencephalic TH+ interneurons synthesize and transport dopamine in vitro

Human iPSC-derived neurons were incubated with a fluorophore-labeled synthetic monoamine. **(A)** TH+ (red) and DDC+ (blue) immunolabeled interneurons (arrowheads) that transported monoamine-imitating fluorophore (green) in vitro. Scale bar represents 10 μm. (**B**) Percentage of neurons that took up the fluorophore and were positive for both the uptake assay and TH. This population is composed of DDC+ (blue) or DDC− (red) interneurons. (**C**) Concentration of dopamine detected by HPLC in the unused (control, Ctrl) cell culture medium, and the conditioned media from LGE and iPSC-derived cultures. Error bars represent SEM. Dunnett's test. *** $P < 0.001$.